

1-1-1998

Formation of Hot Zone By The Application of An Electric Field To Superconducting $\text{Bi}_{1.6}\text{Pb}_{0.4}\text{Sr}_2\text{Ca}_3\text{Cu}_4\text{O}_x$ (2234) Rod

E. YANMAZ

Follow this and additional works at: <https://journals.tubitak.gov.tr/physics>



Part of the [Physics Commons](#)

Recommended Citation

YANMAZ, E. (1998) "Formation of Hot Zone By The Application of An Electric Field To Superconducting $\text{Bi}_{1.6}\text{Pb}_{0.4}\text{Sr}_2\text{Ca}_3\text{Cu}_4\text{O}_x$ (2234) Rod," *Turkish Journal of Physics*: Vol. 22: No. 12, Article 9. Available at: <https://journals.tubitak.gov.tr/physics/vol22/iss12/9>

This Article is brought to you for free and open access by TÜBİTAK Academic Journals. It has been accepted for inclusion in Turkish Journal of Physics by an authorized editor of TÜBİTAK Academic Journals. For more information, please contact academic.publications@tubitak.gov.tr.

Formation of Hot Zone By The Application of An Electric Field To Superconducting $\text{Bi}_{1.6}\text{Pb}_{0.4}\text{Sr}_2\text{Ca}_3\text{Cu}_4\text{O}_x$ (2234) Rod

E. YANMAZ

*Karadeniz Technical University,
Faculty of Arts & Sciences, Department of Physics,
61080 Trabzon-TURKEY*

Received 15.06.1998

Abstract

The formation of hot zone by electric field on superconducting Bi-Pb-Sr-Ca-Cu-O (BSCCO) rods is described. Bulk samples with a nominal composition of $\text{Bi}_{1.6}\text{Pb}_{0.4}\text{Sr}_2\text{Ca}_3\text{Cu}_4\text{O}_x$ (2234) were prepared as rods by a melt casting process. An electrical field was applied to the BSCCO rods and this current caused the resistance of the rod to fall and after a few minutes the initial voltage fell while the current was increased to 2.5A. Under certain conditions, a well-defined hot zone formed at the positive electrode, travelled along the rod and eventually disappeared on reaching the negative electrode. A small increase in the applied current when the zone approached the negative electrode produced another zone at the positive electrode which then exhibited similar behaviour to the first. Reversing the polarity caused the zone to travel in the opposite direction. The rods were characterized by means of microstructural and physical property studies. The results of this method indicates a possible alternative processing route for crystallization of the glassy BSCCO rods and producing superconducting phase.

1. Introduction

Following the discovery of YBCO and BSCCO system superconductors, many studies have been initiated to investigate the preparation, structural identification and enhancement of the transition temperature (T_c), critical current density (J_c) and critical magnetic field (H_c). In the BSCCO system, extensive studies have been continuing on the subjects of increasing the amount of high temperature phase, improving the connectivity between superconducting grains and controlling the the grain diameter and shape, which affect the superconducting properties [1,2]. The melt-quenching and melt-casting procedures

have been applied successfully to the BSCCO system by several authors [3,4]. Glassy material was produced, which was expected to be in a homogeneous state prior to the subsequent crystallization reaction [5]. In previous papers the effect of the applying direct current to cast BSCCO rods of various compositions were reported [6,7]. However, only Osip'yan et al. [8] have applied a dc current to isostatically pressed and sintered YBCO rods. They observed the formation of a hot zone upon passing a dc current through the rod and this zone was observed drifting towards the negative pole. These researchers associated the zoning behaviour to a non-linear temperature dependence of the resistance and with a sharp increase in the resistance during the evolution of oxygen during Joule heating. They pointed out that such a loss would be accompanied by the formation of a high concentration of positively charged oxygen vacancies and they speculated that the mobility of these vacancies could then determine the observed drift of the zone in an electric field. An exchange of oxygen with air was also suggested to play an important role in the process. In this paper, the behaviour of the hot zone formed by electric field, and the structural and physical properties of BSCCO rods are described in detail.

2. Experimental Procedure

2.1. Sample Preparation

The fine powders of Bi_2O_3 , PbO , SrCO_3 , CaO and CuO in the stoichiometric ratios of 1.6:0.4:2:3:4 were well-mixed by milling. The powders of 2234 were subjected to calcination after the milling process. The mixture was then transferred into an alumina crucible and heated at 845°C for 10 hours in an 818 Eurotherm Controller/Programmer muffle furnace. The temperature heating and cooling rates were $2^\circ\text{C}/\text{min}$ and $1^\circ\text{C}/\text{min}$, respectively. The calcined powders were heated in an alumina crucible to 1150°C until the sample was completely molten. During melting process the top of the crucible was covered with an alumina plate in order to prevent the splashing of materials into the furnace and to minimise the loss of materials during the melting. The melts were then poured into a copper mould, which was preheated (at 950°C for 7 min) to avoid cracking in the rods.

The split copper mould has four equal size sections and a hole 5mm diameter was drilled through the mould. During the casting process, the four pieces are joined together by eight screws and heated to an appropriate temperature.

It can be noted that the preheating temperature of the copper mould can not be easily optimised, due to the complexity among the factors of weight, thickness, temperature and holding time. In this work, an appropriate temperature of 950°C and time of 7min was found to be useful for proper casting, as developed by experience. Another very important factor for casting is oxidation of the copper mould during the heating process. If the copper mould is held over 500°C for a long duration (over 7 min.) a thick oxide layer can be formed on the surface of the mould and casting into this mould causes an oxidised surface on the rod which effects the microstructure and physical properties. In order to minimise the oxidation effect, a high temperature and short time is preferred.

2.1. Experimental Set-up

The experimental arrangement is shown schematically in Figure 1. The cast rod was mounted between two brass terminals (Figure 1a) and both ends of the rod were painted by conductive silver paint to reduce the contact resistance. A current was then applied from a dc power supply (60V, 50A) while the rod was held in air. Some experiments have also been carried out in oxygen and argon environments by mounting the rod into a glass tube as shown in Figure 1b. The glass tube was sealed at the ends by a rubber plug and two small holes was drilled for the flowing different gases.

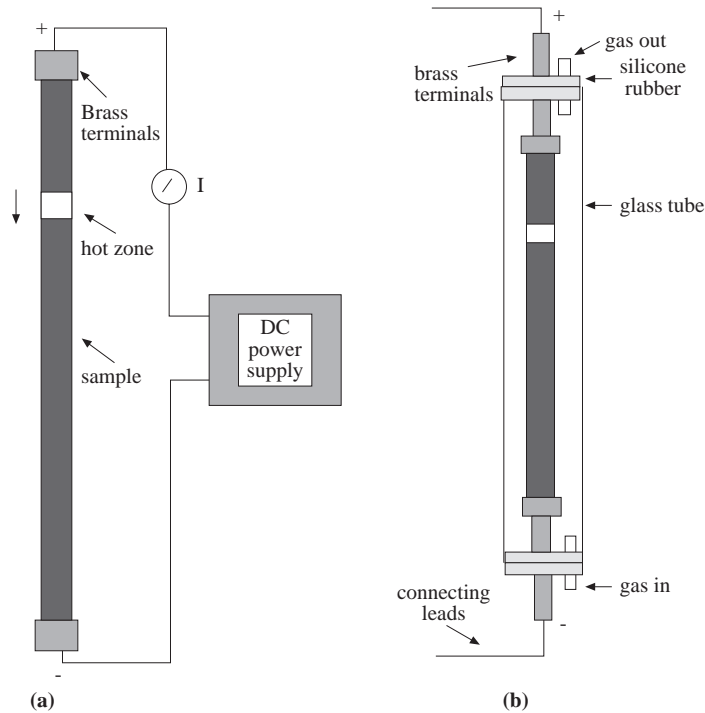


Figure 1. Schematic representation of the experimental set-up (a) in air and (b) in gas environment.

An electric field (60V and 0.3A) was applied to the BSCCO rods and this current caused the resistance of the rod to fall and after 1 to 2 minutes the initial voltage fell to 20V while the current was increased to 2.5A. Under certain conditions, a well-defined hot zone formed at the positive electrode and this travelled along the rod and eventually disappeared on reaching the negative electrode. A small increase in the applied current when the zone approached the negative electrode produced another zone at the positive electrode which then exhibited similar behaviour to the first. In order to investigate the effects of DCZ on the microstructure of the rod, a hot zone was arrested in the middle

of the rod on a first pass by switching off the current. Therefore, it was decided that four regions could be examined for microstructural investigation, and these are the \pm ev (contacts), zone pass, zone and un-zoned regions, as indicated schematically in Figure 2.

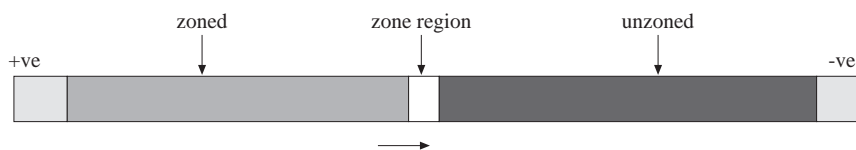


Figure 2. Schematic representation of a BSCCO rod treated by direct current zoning method(DCZ).

Additionally, we have propagated consecutive single zones through the same bar, up to six times, each subsequent operation requiring a slight increase in the applied current. The number of zones can be increased further by carefully controlling the current, otherwise the sample can easily melt at the zone region.

It is also possible to heat the whole rod uniformly by applying a current just below that required to produce a zone. For this process, a current of 2A was applied to the rods treated by DCZ for various times in air.

The microstructure of rods was studied by optical and scanning electron microscopy (SEM). Phase analysis was carried out by EDX and XRD. A Faraday magnetometer was used to measure dc susceptibility at room temperature. Superconducting transition temperature (T_c) of samples were determined by low temperature ac. susceptibility measurements.

3. Results and Discussion

3.1 Microstructure of 2234 Rod

A SEM micrograph of melt cast rod is shown in Figure 3. The micrograph of 2234 composition indicates glass structure with some crystalline precipitates. At least four different phases can be observed: the amorphous matrix, long needles embedded in an amorphous mass, a rounded dark phase and some dendritic phase mostly formed around the rounded phase.

An EDX analysis was performed in order to determine the crystalline phases present in the 2234 composition. The EDX results revealed that the amorphous matrix is Bi-rich, the long needle phase is $\text{Sr}_{14-x}\text{Ca}_x\text{Cu}_{24}\text{O}_y$ $x = 6.5 - 7$, which is lacking in Bi and Pb and enriched in Cu, and the rounded phase is 98 atomic percent CaO phase. The semiconducting $\text{Sr}_{14-x}\text{Ca}_x\text{Cu}_{24}\text{O}_y$ phase has been reported by McCarron et al [9] and they suggested that the semiconducting needle-like crystals remain in the range of $0 < x < 8$. The dendritic phase was determined to be a Cu-rich phase. It can be seen from micrograph that the size of the dendritic phase is very small, and could be smaller than the electron beam spot; this suggests, possibly that, some elements will be detected

around the dendritic phase, therefore, a considerable error can be expected on the data of the dendritic phase. The EDX qualitative results of the present crystalline phases in the as-cast 2234 rod is shown in Figure 4.

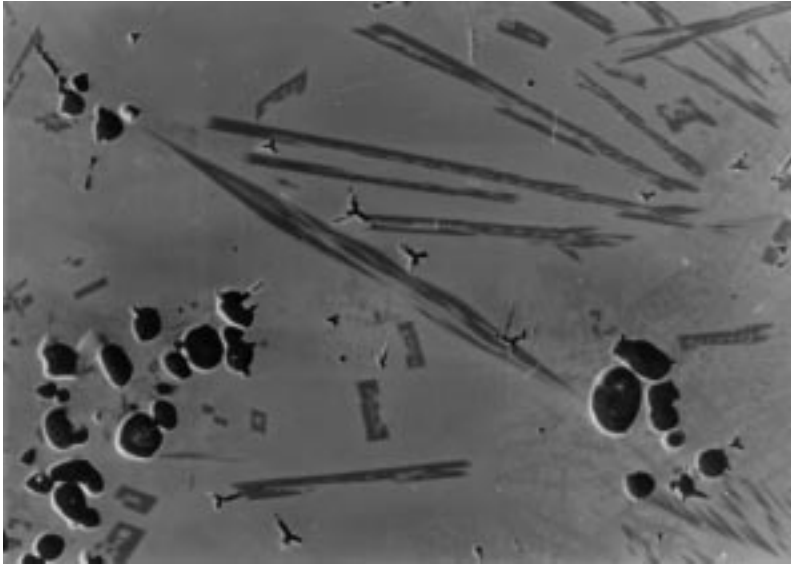


Figure 3. Shows the SEM image of a melt-cast 2234 rod. As can be seen, there are a number of phases in an amorphous matrix, including long needles, rounded and some dendritic phases formed after solidification process.

3.2. Direct Current Zoning (DCZ)

Photographs of the position of the hot zones in BSCCO rods are shown in Figure 5. Initial application of the maximum voltage (60 V) resulted in a current of 0.3 A passing through the rod. This caused the resistance of the rod to fall and after 1 to 2 minutes a steady state was established and the voltage required to maintain this current fell to 20 V. The surface colour of the rod changed after around 2 minutes by passing the initial current, and this indicates that the rod was heated up to a certain temperature. On increasing the current to 2.5 A, a well defined hot zone ($840(\pm 20)^{\circ}\text{C}$) formed at the positive electrode (1st photo). This zone travelled along the rod (3rd photo) and eventually disappeared on reaching the negative electrode leaving a corrugated surface on the rod as shown in Figure 6. The speed of this first zone could be increased to 2 mm/s by increasing the current to a maximum value of approximately 3 A. Above this current, the sample started to melt in the zone region. The zone could be arrested and then eliminated by reducing the current progressively; on subsequent application of the current the zone reappeared at the position on the rod where it had stopped. It is worth noting from Figure 5 that the leading edge of the zone is particularly sharp, indicating

an abrupt change in the resistive properties of the rod at this zone/matrix interface. Reversing the current caused the zone to travel in the opposite direction. The zoning behaviour observed in BSCCO rod was referred to as Direct Current Zoning (DCZ).

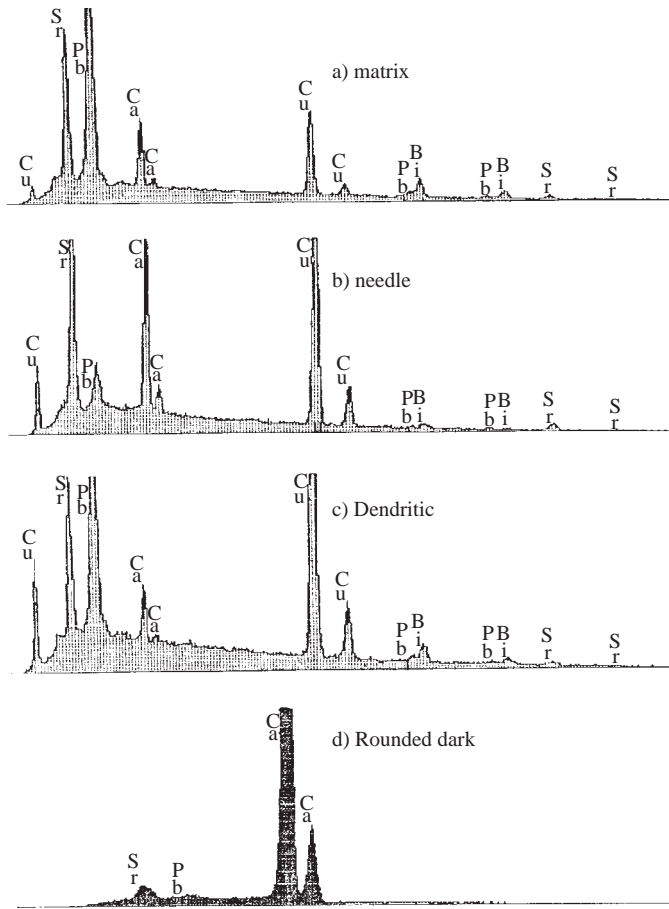


Figure 4. EDX qualitative results of the present crystalline phases in the as-cast 2234 rod.

A small increase in the applied current of 0.2 A when the first zone approached the negative electrode (Figure 5c) produced another zone at the positive electrode which then exhibited similar behaviour to the first, as shown in Figure 5d, 5e and 5f. Several consecutive single zones (up to six) have been propagated through the same bar, each subsequent operation requiring a slight increase in the applied current. No evidence was found that these operations could not be continued indefinitely by further incremental steps in the current.

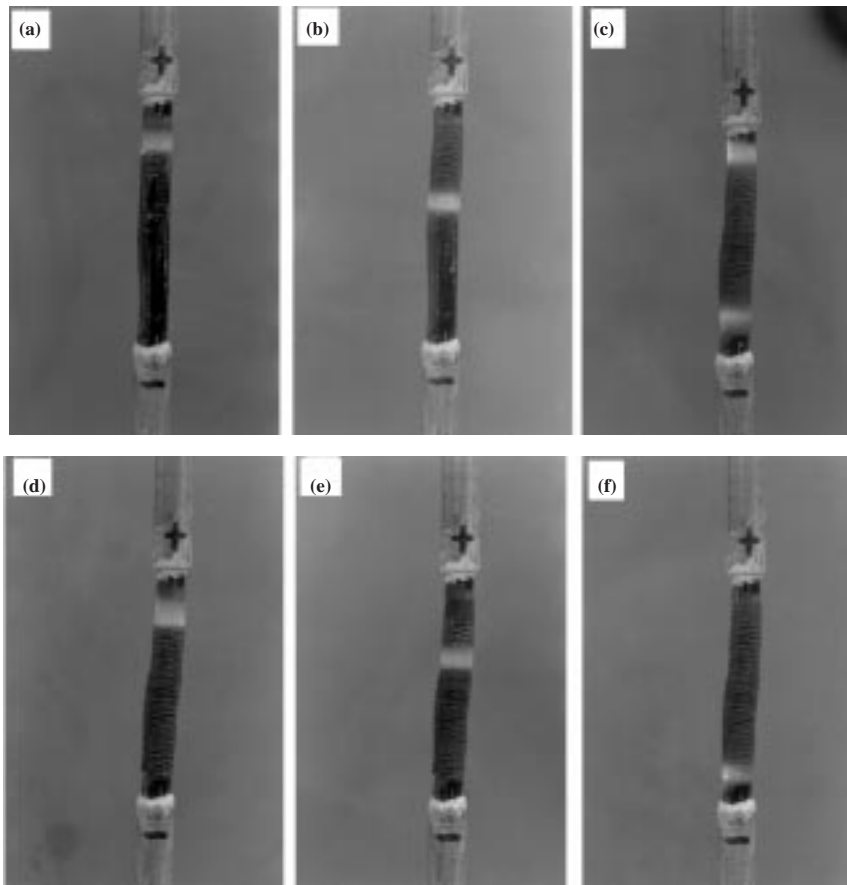


Figure 5.The creation and movement of hot zone along the bar.

3.3. Microstructural Investigation of 2234 Rod Treated By DCZ Method

In order to investigate the effect of DCZ on the changes of microstructure of a rod, a hot zone was arrested in the middle of the rod on a first pass by switching off the current and the microstructural investigations were carried out on the four different parts of rod, as illustrated in Figure 2: zone region, zoned and unzoned regions and the \pm ve electrodes.

The microstructure of a longitudinal section of the quenched zone region is shown in Figure 7a. The SEM micrograph indicates that there is a sharp interface between the zoned and unzoned material which is consistent with the observation of the zone in Figure 5, and suggests a recrystallisation and/or constitutional transformation front moving through the rod. It can also be seen that after zoning, the microstructure of the rod (R in Figure 7a) has changed radically from that of the initial cast state (L in Figure 7a). The interface and the zone region immediately behind it consist of a fine mixture

of phases and is interspersed with rounded particles of free Cu (x1) as shown in Figure 7b. The other phases in the zone region were determined by EDX analysis to be CaO, Bi-rich phase and Bi-Cu rich phases.



Figure 6. A well-defined hot zone forms at positive electrode and travelled along the rod and disappeared on reaching the negative electrode leaving a corrugated surface on the rod.

Contrast with the SEM micrograph of a single zoned rod, as shown in Figure 7c. The micrographs clearly indicated that crystallisation has occurred and some new phases formed after a single zone was passed. The single zone passed rod showed rectangular needles and dark rounded phases with a finely distributed grey phase. It is thought that the finely distributed grey phase formed from the crystallised glass matrix. Growth of the rectangular needles and a decrease of the dark rounded phases can also be observed by increasing the number of zone passes. Consequently, the micrographs reveal that the initial (cast state) structure of the rod has drastically changed by zone passes and resulted in a crystallised rod.

The EDX result indicated that the rectangular needles contain around 4% Bi element. But, it is important to note that the rectangular needles are different from the needles observed in the cast state. This may suggest that the initial needle phases reacted with the matrix during crystallisation and formed new types of needles with different atomic percentage of elements.

The powders obtained from the zoned rods have been examined by x-ray diffraction ($\text{Cu-K}\alpha$ analysis and the patterns are presented in Figure 8. The Figure shows the cast state and exhibits a large halo which is typical of amorphous material with some crystalline phases. These phases indicated on the peaks. As mentioned before, when a zone is passed through the rod, recrystallisation takes place in the glass part of rod. Therefore, the x-ray patterns are the evidence of structure changes by zoning. The patterns indicate a number of peaks and they were determined to be (o) 2201 very low- T_c phase (10-20K) and the others attributed to need CaO and CuO which were determined by EDX analysis. Consequently, the most important result seen here is the formation of one of the superconducting structures by the application of DCZ method.

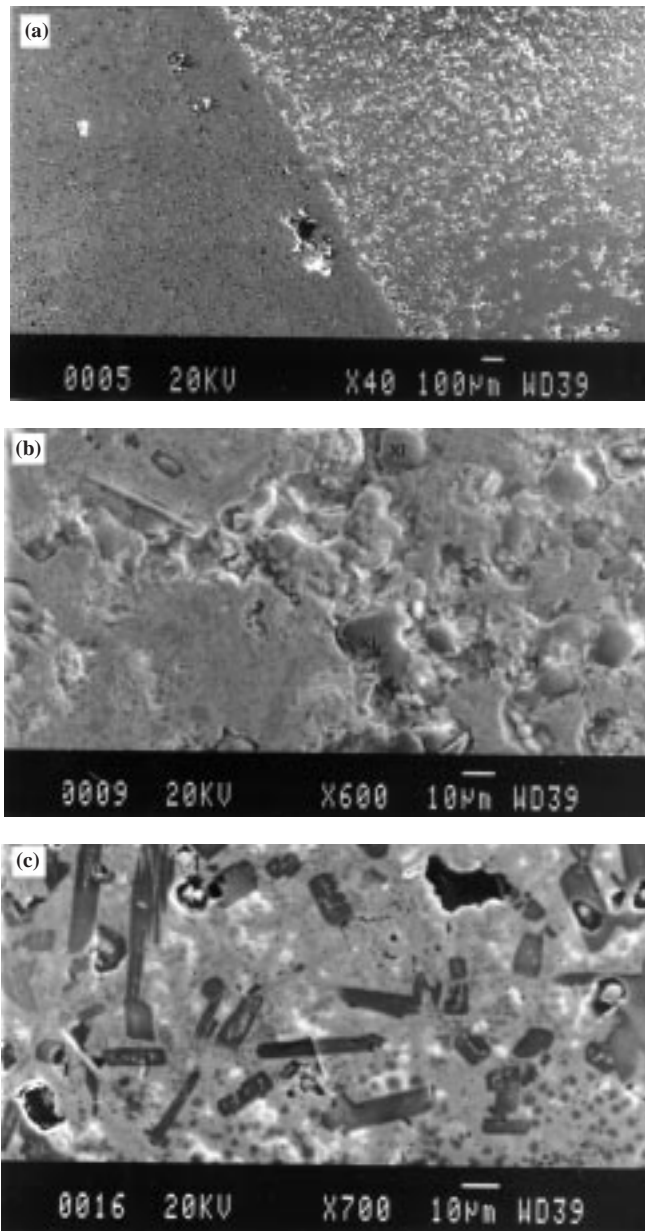


Figure 7. The SEM images of zone region showing (a) a sharp interface between zoned and unzoned materials, (b) presence of phases in the zone region and (c) microstructure of a single zone passed BSCCO rod.

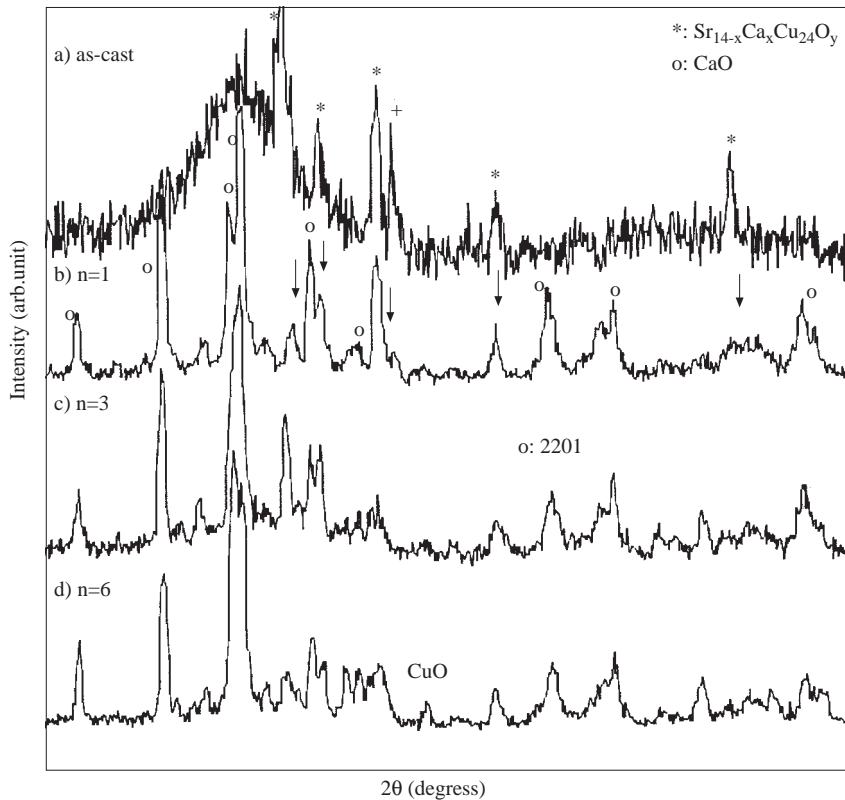


Figure 8. Room temperature XRD patterns taken from (a) as-cast and (b)-(d) number of zoned materials.

3.4 Unzoned Region

The optical images of the unzoned part of the cast rod are illustrated in Figure 9. The micrograph clearly indicates that the initial crystalline phases (long needles and rounded phases) still remain in the unzoned region even though the temperature of the rod had risen prior to the passage of the first zone. But, the micrographs reveal more dendritic phase within the structure which was formed by the temperature rise. It is thought that the amorphous matrix crystallised with this temperature rise and resulted in the growth of the dendritic phase.

3.5 \pm VE Contact Regions

As we saw in Figure 7c, the structure of a cast rod has changed radically from that of the initial cast state after a zone pass. The interface and the zone region immediately behind it consist of a fine mixture of phases and is interspersed with rounded particles of

free Cu. However, after a few zone passes, a large free-Cu region was observed at the -ve electrode. It was found that the amount of free-Cu at the -ve electrode depended on the number of zone passes, that is, free-Cu increased with the number of zones. However, it is not clear at this stage what the mechanism of the zone formation is and the mobility of the zone. At this moment, we may propose that the copper atoms are migrating from +ve electrode to the -ve electrode under a dc field.

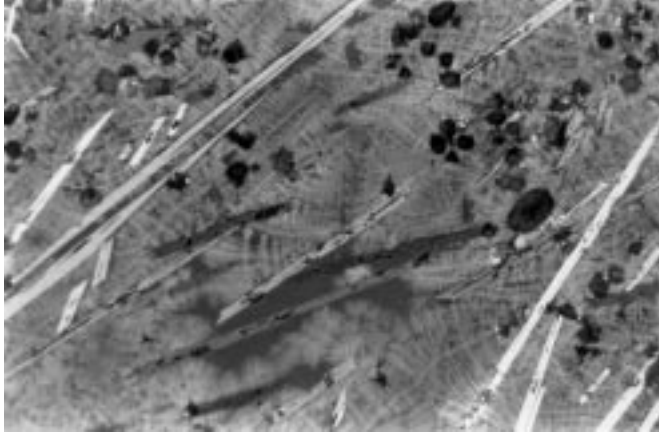


Figure 9. An optical image of unzoned part of a cast rod. The micrograph indicates that the initial crystalline phases (long needles and rounded) still remain in the unzoned region.

3.6. Magnetic Measurements

In order to investigate the effect of the DCZ process on the magnetic properties of a cast rod, room temperature magnetic susceptibility measurements on as-cast, half zoned and three times zoned rods were performed on a Faraday balance.

The magnetic susceptibility results as a function of rod position are given in Figure 10a. It was found that the average susceptibility of a cast rod was around 5×10^{-7} emu/gOe. The first data point, which corresponds to the top of the rod in the cast state, has a slightly higher value. But, the values for all data points are very close to each other and suggest that the cast sample has got almost a uniform structure. In the case of the first value, it is thought that the solidification rate between top and bottom of the rod during casting could be slightly different, and this may result in some differences in the magnetic susceptibility.

In the case of half zoned rod shown in Figure 10b, the magnetic susceptibility signal in the different parts of the rod was found to be very different. Position 1 corresponds to the +ve electrode, and position 2 corresponds to the position immediately next to the +ve electrode, while positions from 3 to 5 represents the zone passed region. The positions 5 to 6, position 7, positions 8 to 10 and position 11 correspond to locations immediately behind the zone, zone, unzoned and -ve electrode regions, respectively. The

susceptibility in the zone region (position 7) showed a negative signal which corresponds to diamagnetic behaviour, and this is consistent with the evidence of the presence of free-Cu in the zone region. It was also noted that the susceptibility signal at the +ve electrode had the highest value (position 1) and it was thought that the time zone spent at this point was longer and resulted in some differences in the magnetic behaviour.

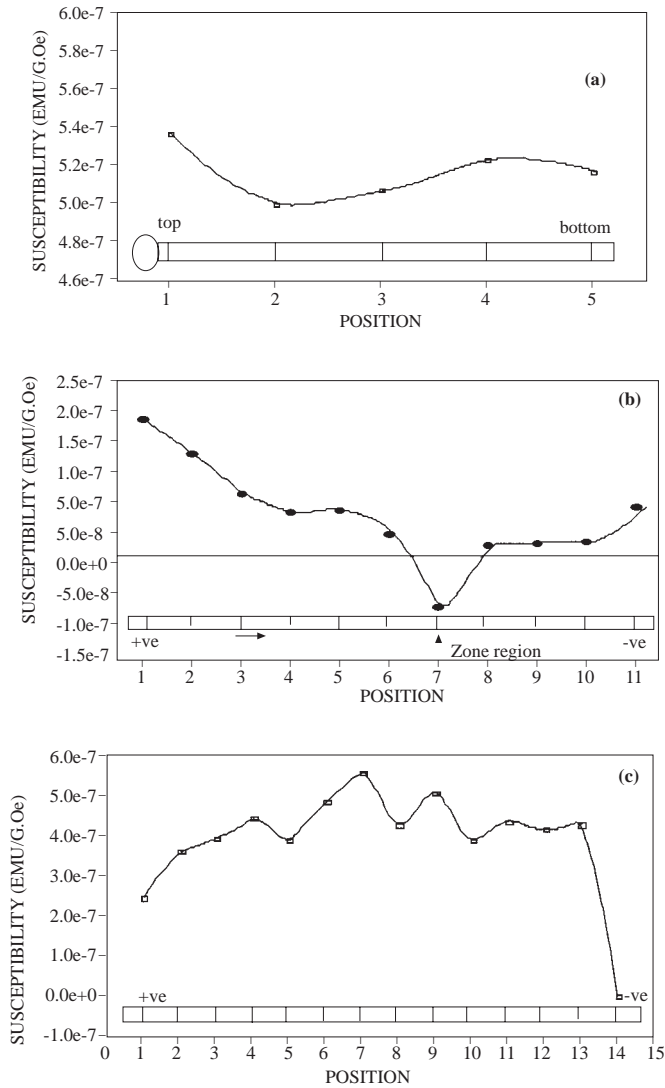


Figure 10. Variation of magnetic susceptibility of (a) as-cast, (b) half zoned and (c) three times zoned rods. The error for this measurement is around $\pm 2.0 \times 10^{-9}$ emu/gOe.

The magnetic susceptibility signal of the zone passed region (positions 3 to 5) increased with an increase in the number of zone passes, as shown in Figure 10c. This suggests that every zone passage create a more uniform crystalline structure. But, it is very important to note that the susceptibility values at the \pm ev electrodes after three zone passes became very small, and even became negative at the -ve electrode (position 14). It was thought that this is a confirmation of the migration of Cu atoms to the -ve electrode.

3.7 DCZ Process on 2234 Rods in a Different Environment

Up to now, the behaviour of the DCZ process was investigated in air. Investigations were also carried out in argon and in oxygen environments. The experimental set up for this measurement is shown in Figure 1b. The preliminary observations on DCZ behaviour in argon atmosphere indicated that the zone took longer to form and appeared to be immobile. The zone also became progressively hotter with time and eventually melting occurred with consequent separation of the rod in the region of the zone. Another important observation in argon is the effective volume change. The geometry of rod became very rough at the zone region under argon. When the argon was quickly replaced with the oxygen, it was found that the zone became narrow and sharper at the interface in a few minutes and started to move towards to the -ve electrode. If the oxygen is again replaced by argon, the zone became large and immobile again. Therefore, these results indicate that the DCZ process is strongly dependent on the sample composition and environment. At the moment the mechanism of DCZ process is not clear, but, there is a very clear indication that oxygen is a key element in this process.

3.8. Direct Current Annealing (DCA)

It is also possible to heat the whole bar uniformly by applying a current just below that required to produce a zone. This process is referred to as Direct Current Annealing (DCA). A BSCCO rod was heated to a certain temperature by applying a constant current (2A). The rod temperature was estimated to be $800 (\pm 20)^\circ\text{C}$ by an optical pyrometer. It is noticed that a small area near the negative electrode is slightly more heated, but after a time that part of the rod also exhibited the same red heat as the other parts. This suggests that the localised resistance of the rod becomes more uniform with time during the formation of new phases.

A number of DCZ rods were annealed for various times by this method and a list of samples is given in Table1. The temperature dependence of the normalised ac-susceptibility of samples 1 to 5 is shown in Figure 11. The ac-susceptibility measurements indicate a superconducting transition with an onset temperature of 80K which becomes progressively sharper from samples 1 to 5. This Figure indicates that the onset temperatures ($T_{c,\text{onset}}$) for the samples 1 to 4 is almost the same (80K) while it increased to 105K for sample 5. The zero resistance transition ($T_{c,\text{zero}}$) increases with increasing annealing time for DCA samples and the $T_{c,\text{zero}}$ for these samples were found to be 30K, 72K and 102K. Sample 4 also indicates a small transition step at around 102K which corresponds to transition temperature of high- T_c phase. Therefore, this is an indication of the pres-

ence of a high- T_c phase in the sample 4. The onset and zero transition temperature of sample 5 indicates that the high- T_c phase (2223) can be obtained by further annealing of sample in a muffle furnace at a temperature of 850°C after the combination of DCZ and DCA processes.

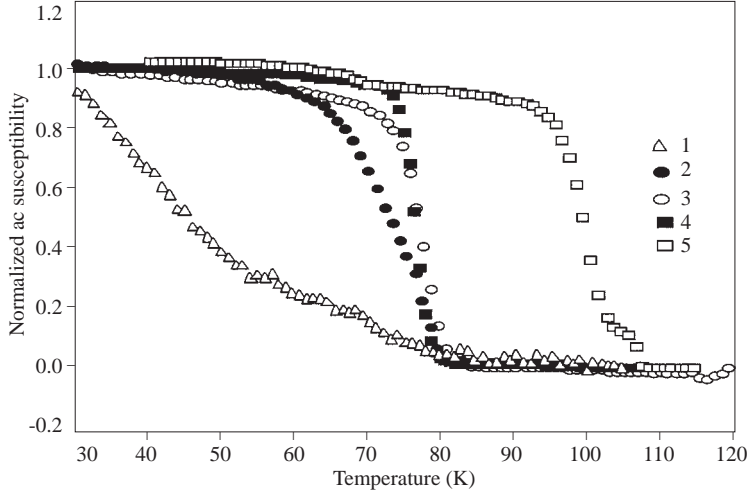


Figure 11. Temperature dependencies of ac susceptibility for DCA samples (see Table 1.)

Table 1. Samples prepared by direct current processing. All samples have been zoned six times then annealed by passing a current of 2A through them (DCA) for the periods indicated. Sample 5 was removed from the zoning rig after a three hour anneal and further annealed in a muffle furnace in air for 50 hours at 850°C.

Sample	Specification
1	6 zone pass+10h annealing at a constant current (2A)
2	6 zone pass+25h annealing at a constant current (2A)
3	6 zone pass+50h annealing at a constant current (2A)
4	6 zone pass+3h annealing at a constant current (2A)+ 50h annealing at 850°C in a muffle furnace

3.9. Summary of DCZ and DCA Process

According to the results shown so far, the recrystallisation of glassy melt-cast rods can be easily performed by the DCZ process and a high proportion of the 2212 phase with a sharp T_c at 80K could be obtained by the combination of the DCZ process with subsequent DCA treatment. These results suggest that one of the superconducting phases, especially the 2212 phase, can be produced by these methods using melt-cast precursor rods. The temperature measurements, using optical pyrometer, indicated that the zone region was 850 (± 20)°C and a uniformly heated rod (DCA) was 800(± 20)°C. It is also

well known that the formation of high- T_c phase (2223) occurs above 830C. Therefore, we may say that the temperature of uniformly heated rod is not enough to form the high- T_c phase. In order to hold the temperature close to 850°C, the applied current and the environment during processing must be controlled to achieve the optimum superconducting properties.

Preliminary observations on DCZ behaviour in BSCCO rods in an argon environment indicated that, compared with the same conditions in air, the zone took longer to form and appeared to be immobile. The zone also became progressively hotter with time and eventually melting occurred with the consequent separation of the rod in the region of the zone. It was also observed that, when oxygen was flowed immediately after argon, the zone become narrow and started to move in the normal direction (from positive to negative electrode). It is not clear at this stage whether significant loss of oxygen at high temperatures occurs in the case of BSSCO. However, the movement of oxygen ions under the influence of the electric field is thought to be an important factor because very different behaviours observed in air and argon.

References

- [1] B. Hensel, J.C. Grivel, A. Jeremie, A. Perin, A. Pollini, and R. Flükiger, *Physica C*, 205 (1993) 329.
- [2] F. Zhanguo and Chunlin, *J. Less-Common Met.*, 152 (1989) 45.
- [3] T. Komatsu, N. Tamoto, R. Sato, K. Matusita, K. Sawada and T. Yamashita, *Jpn.J. Appl.Phys.*, 30 (1A) (1991) L21.
- [4] J. Bock and E. Preisler, *Solid State Commun.*, 72(5) (1989) 453.
- [5] E. Yanmaz, J.S. Abell and I.R. Harris, *Physica C*, 185-189 (1991) 2415.
- [6] E. Yanmaz, J.S. Abell and I.R. Harris, *J. Alloys and Compounds*, 185 (1992) 311.
- [7] E. Yanmaz, J.S. Abell and I.R. Harris, *J. Alloys and Compounds*, 195 (1993) 39.
- [8] Osip'yan, Y.A., Nikolaev, R.K., Siderov, N.S., Boborov, V.S. and Tosi, V.S., *JETP Lett.*47, 310, 1988.
- [9] E.M. McCarron, M.A. Subramanian, J.C. Calabrese and R.L. Harlow, *Mater.Res.Bull.*, 23 (1988) 1355.